

Convergence of the chiral expansion in two-flavor lattice QCD

J. Noaki,¹ S. Aoki,^{2,3} T.W. Chiu,⁴ H. Fukaya,^{5,1} S. Hashimoto,^{1,6} T.H. Hsieh,⁷
T. Kaneko,^{1,6} H. Matsufuru,¹ T. Onogi,⁸ E. Shintani,¹ and N. Yamada^{1,6}

(JLQCD and TWQCD Collaborations)

¹ *High Energy Accelerator Research Organization (KEK), Tsukuba 305-0801, Japan*

² *Graduate School of Pure and Applied Sciences,
University of Tsukuba, Tsukuba 305-8571, Japan*

³ *Riken BNL Research Center, Upton, NY 11973, USA*

⁴ *Physics Department, Center for Theoretical Sciences, and National Center
for Theoretical Sciences, National Taiwan University, Taipei 10617, Taiwan*

⁵ *The Niels Bohr Institute, The Niels Bohr International
Academy, Blegdamsvej 17 DK-2100 Copenhagen Ø Denmark*

⁶ *School of High Energy Accelerator Science, The Graduate University
for Advanced Studies (Sokendai), Tsukuba 305-0801, Japan*

⁷ *Research Center for Applied Sciences, Academia Sinica, Taipei 115, Taiwan*

⁸ *Yukawa Institute for Theoretical Physics, Kyoto University, Kyoto 606-8502, Japan*

(Dated: March 15, 2019)

Abstract

We test the convergence property of the chiral perturbation theory (ChPT) using a lattice QCD calculation of pion mass and decay constant with two dynamical quark flavors. The lattice calculation is performed using the overlap fermion formulation, which realizes exact chiral symmetry at finite lattice spacing. By comparing various expansion prescriptions, we find that the chiral expansion is well saturated at the next-to-leading order (NLO) for pions lighter than ~ 450 MeV. Better convergence behavior is found in particular for a resummed expansion parameter ξ , with which the lattice data in the pion mass region $290\sim 750$ MeV can be fitted well with the next-to-next-to-leading order (NNLO) formulae. We obtain the results in two-flavor QCD for the low energy constants \bar{l}_3 and \bar{l}_4 as well as the pion decay constant, the chiral condensate, and the average up and down quark mass.

PACS numbers: 11.15.Ha, 12.38.Gc

Chiral perturbation theory (ChPT) is a powerful tool to analyze the dynamics of low energy pions [1]. The expansion parameter in ChPT is the pion mass (or momentum) divided by the typical scale of the underlying theory such as Quantum Chromodynamics (QCD). Good convergence of the chiral expansion is observed for physical pions in the analysis including the next-to-next-to-leading order (NNLO) for the pion-pion scattering [2], for instance. In the kaon mass region, on the other hand, the validity of ChPT is not obvious and in fact an important issue in many phenomenological applications.

Lattice QCD calculation can, in principle, be used for a detailed test of the convergence property of ChPT, as one can freely vary the quark mass, typically in the range $m_s/5 \sim m_s$ with m_s the physical strange quark mass. However, such a direct test has been difficult, since the lattice regularization of the quark action explicitly violates flavor and/or chiral symmetry in the conventional formulations, such as the Wilson and staggered fermions. One then has to introduce additional terms with unknown parameters in order to describe those violations in ChPT, hence the test is obscured.

The aim of this article is to provide a direct comparison between the ChPT predictions and lattice QCD calculations, using the overlap fermion formulation on the lattice, that preserves exact chiral symmetry at finite lattice spacing a [3, 4]. With the exact chiral symmetry, the continuum ChPT can be directly used to describe the lattice data; the discretization error of $\mathcal{O}(a^2)$ only affects the value of the Low Energy Constants (LECs) determined by fitting the lattice data. We calculate the pion mass and decay constant in two-flavor QCD, for which the NNLO calculations are available in ChPT [5]. A preliminary report of this work is found in [6].

Lattice simulations are performed on a $L_s^3 \times L_t = 16^3 \times 32$ lattice at a lattice spacing $a = 0.1184(3)(21)$ fm determined with an input $r_0 = 0.49$ fm, the Sommer scale defined for the heavy quark potential. At six different sea quark masses m_{sea} , covering the pion mass region $290 \text{ MeV} \lesssim m_\pi \lesssim 750 \text{ MeV}$, we generate 10,000 trajectories, among which the calculation of the pion correlator is carried out at every 20 trajectories. For further details of the simulation we refer [7].

In the calculation of the pion correlator, we computed in advance the lowest 50 conjugate pairs of eigenmode of the overlap-Dirac operator on each gauge configuration and stored on the disk. Then, by using the eigenmodes to construct a preconditioner, the inversion of the overlap-Dirac operator can be done with only $\approx 15\%$ of the CPU time of the full

calculation. The low-modes are also used to improve the statistical accuracy by averaging their contribution to the correlators over 32 source points distributed in each time slice. The correlators are calculated with a point source and a smeared source; the pion mass m_π and decay constant f_π are obtained from a simultaneous fit of them.

The pion decay constant f_π is defined through $\langle 0 | \mathcal{A}_\mu | \pi(p) \rangle = i f_\pi p_\mu$, where \mathcal{A}_μ is the (continuum) iso-triplet axial-vector current. Instead of \mathcal{A}_μ , we calculate the matrix element of pseudo-scalar density P^{lat} on the lattice using the PCAC relation $\partial_\mu \mathcal{A}_\mu = 2m_q^{\text{lat}} P^{\text{lat}}$ with m_q^{lat} the bare quark mass. Since the combination $m_q^{\text{lat}} P^{\text{lat}}$ is not renormalized, no renormalization factor is needed in the calculation of f_π . This is possible only when the chiral symmetry is exact. The renormalization factor for the quark mass $m_q = Z_m^{\overline{\text{MS}}}(2 \text{ GeV}) m_q^{\text{lat}}$ is calculated non-perturbatively through the RI/MOM scheme, with which the renormalization condition is applied at some off-shell momentum for propagators and vertex functions. Such a non-perturbative calculation suffers from the non-trivial quark mass dependence of the chiral condensate. By using the calculated low-modes explicitly, we are able to control the mass dependence to determine $Z_m^{\text{RI/MOM}}$ more reliably. In the chiral limit, we obtain $Z_m^{\overline{\text{MS}}}(2 \text{ GeV}) = 0.838(14)(03)$, where the second error arises from a subtraction of power divergence from the chiral condensate. The details of this calculation will be given elsewhere.

Since our numerical simulation is done on a finite volume lattice with $m_\pi L_s \simeq 2.9$ for the lightest sea quark, the finite volume effect could be significant. We make a correction for the finite volume effect using the estimate within ChPT calculated up to $\mathcal{O}(m_\pi^4/(4\pi f_\pi)^4)$ [8]. The size of the corrections for m_π^2 and f_π is about 5% for the lightest pion mass and exponentially suppressed for heavier data points. In addition, there is a correction due to fixing the global topological charge in our simulation [7, 9]. This leads to a finite volume effect of $\mathcal{O}(1/V)$ with V the physical space-time volume. The correction is calculable within ChPT [10, 11] depending on the value of topological susceptibility χ_t , which we calculated in [12]. At NLO, the correction for m_π^2 is similar in magnitude but opposite in sign to the ordinary finite volume effect at the lightest pion mass, and thus almost cancels. For f_π the finite volume effect due to the fixed topology starts at NLO and therefore is a subdominant effect. Note that the LECs appear in the calculation of these correction factors. We use their phenomenological values at the scale of physical (charged) pion mass $m_{\pi^+} = 139.6 \text{ MeV}$: $\bar{l}_1^{\text{phys}} = -0.4 \pm 0.6$, $\bar{l}_2^{\text{phys}} = 4.3 \pm 0.1$, $\bar{l}_4^{\text{phys}} = 4.4 \pm 0.2$, determined at the NNLO [2] and $\bar{l}_3^{\text{phys}} = 2.9 \pm 2.4$. The errors in these values are reflected in the following analysis assuming

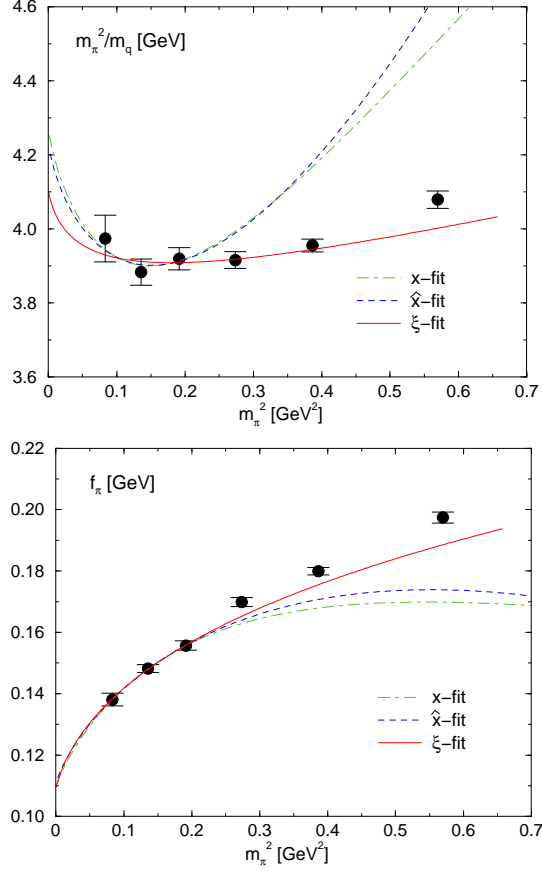


FIG. 1: Comparison of the chiral fits including the NLO terms for m_π^2/m_q (top) and f_π (bottom). Fit curves to three lightest data points obtained with different choices of the expansion parameter (x , \hat{x} , and ξ) are shown as a function of m_π^2 .

a gaussian distribution.

After applying the finite volume corrections, we first analyze the numerical data for m_π^2/m_q and f_π using the ChPT formulae at NLO,

$$m_\pi^2/m_q = 2B(1 + x \ln x) + c_3x, \quad (1)$$

$$f_\pi = f(1 - 2x \ln x) + c_4x, \quad (2)$$

where f is the pion decay constant in the chiral limit and B is related to the chiral condensate. Here the expansion is made in terms of $x \equiv 2Bm_q/(4\pi f)^2$. The parameters c_3 and c_4 are related to the LECs \bar{l}_3^{phys} and \bar{l}_4^{phys} , respectively. At NLO, *i.e.* $\mathcal{O}(x)$, these expressions are unchanged when one replaces the expansion parameter x by $\hat{x} \equiv m_\pi^2/(4\pi f)^2$ or $\xi \equiv m_\pi^2/(4\pi f_\pi)^2$, where m_π and f_π denote those at a finite quark mass. Therefore, in a small enough pion mass region the three expansion parameters should describe the lattice data

equally well.

Three fit curves (x -fit, \hat{x} -fit, and ξ -fit) for the three lightest pion mass points ($m_\pi \lesssim 450$ MeV) are shown in Figure 1 as a function of m_π^2 . From the plot we observe that the different expansion parameters seem to describe the three lightest points equally well; the χ^2/dof is below 0.35 except for m_π^2/m_q with the ξ -fit, for which χ^2/dof is 1.29. (We note that χ^2/dof does not have the precise meaning for the x - and \hat{x} -fits, because m_π^2/m_q and f_π are fitted simultaneously as the fit parameters enter the definition of x (or \hat{x}) while the correlation among the two quantities is not taken into account. It still indicates the quality of the fit to some extent.) Between the x - and \hat{x} -fit, all of the resulting fit parameters are consistent. Among them, B and f , the LECs at the leading order ChPT, are also consistent with the ξ -fit. This indicates that the NLO formulae successfully describes the data.

The agreement among the different expansion prescriptions is lost (deviation is greater than 3σ) when we extend the fit range to include the next lightest data point at $m_\pi \simeq 520$ MeV. We, therefore, conclude that for these quantities the NLO ChPT may be safely applied only below ≈ 450 MeV.

Another important observation from Figure 1 is that only the ξ -fit reasonably describes the data beyond the fitted region. With the x - and \hat{x} -fits the curvature due to the chiral logarithm is too strong to accommodate the heavier data points. In fact, values of the LECs with the x - and \hat{x} -fits are more sensitive to the fit range than the ξ -fit. This is because f , which is significantly smaller than f_π of our data, enters in the definition of the expansion parameter. Qualitatively, by replacing m_q and f by m_π^2 and f_π the higher loop effects in ChPT are effectively resummed and the convergence of the chiral expansion is improved.

We then extend the analysis to include the NNLO terms. Since we found that the ξ -fit is the best to describe the data, we only consider the expansion in terms of ξ in the following. At the NNLO, the formulae are available as [2]

$$\begin{aligned}
m_\pi^2/m_q = & 2B \left[1 + \xi \ln \xi + \frac{7}{2}(\xi \ln \xi)^2 \right. \\
& + \left(\frac{c_4}{2f} - \frac{4}{3}(\tilde{l}^{\text{phys}} + 16) \right) \xi^2 \ln \xi \Big] \\
& + c_3 \xi (1 - 9\xi \ln \xi) + \alpha \xi^2,
\end{aligned} \tag{3}$$

$$\begin{aligned}
f_\pi = & f \left[1 - 2\xi \ln \xi + 5(\xi \ln \xi)^2 + \frac{3}{2}(\tilde{l}^{\text{phys}} + \frac{53}{2})\xi^2 \ln \xi \right] \\
& + c_4 \xi (1 - 10\xi \ln \xi) + \beta \xi^2.
\end{aligned} \tag{4}$$

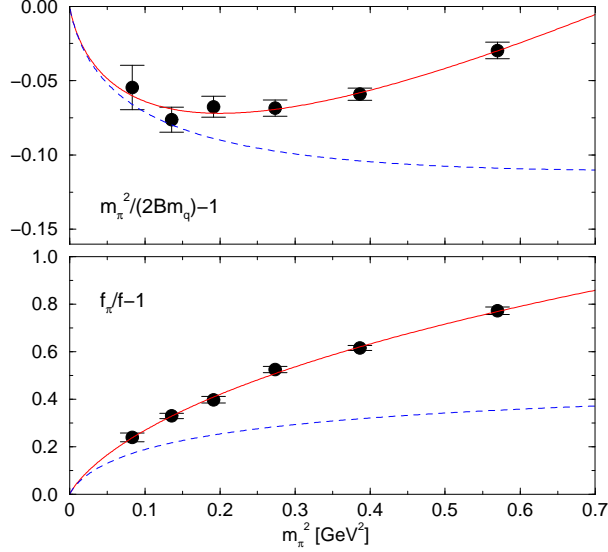


FIG. 2: NNLO chiral fits using all the data points for m_π^2/m_q (top) and f_π (bottom). Data are normalized by the value in the chiral limit. Solid curves show the NNLO fit, and the truncated expansions at NLO are shown by dashed curves.

In the terms of $\xi^2 \ln \xi$, the LECs at NLO appear: $\tilde{l}^{\text{phys}} \equiv 7\bar{l}_1^{\text{phys}} + 8\bar{l}_2^{\text{phys}} - 15 \ln(4\pi f_\pi^{\text{phys}}/m_{\pi^+})^2$, where $f_\pi^{\text{phys}} = 130.7$ MeV. We input the phenomenological estimate $\tilde{l}^{\text{phys}} = -42.4 \pm 4.3$ to the fit. Since the data are not precise enough to discriminate between $\xi^2 \ln \xi$ and ξ^2 in the given region of ξ ($0.028 \sim 0.093$), fit parameters α and β partially absorb the uncertainty in \tilde{l}^{phys} . In fact, our final results for the LECs is insensitive to \tilde{l}^{phys} .

In Figure 2, we show the NNLO fits using all the data points (solid curves). In these plots m_π^2/m_q and f_π are normalized by their values in the chiral limit. As expected from the good convergence of the ξ -fit even at NLO, the NNLO formulae nicely describe the lattice data in the whole data region. We also draw a truncation at the NLO level (dashed curves) but using the same fit parameters. The difference between the NLO truncated curves and the NLO fit curves to the three lightest data points (Figure 1) is explained by the presence of the terms $\xi(1 - 9\xi \ln \xi)$ and $\xi(1 - 10\xi \ln \xi)$ in (3) and (4), respectively. Since the factors $(1 - 9\xi \ln \xi)$ and $(1 - 10\xi \ln \xi)$ are significantly larger than 1 in the data region, the resulting fit parameters c_3 and c_4 in the NNLO formulae are much lower than those of the NLO fits. This indicates that the determination of the NLO LECs is quite sensitive to whether the NNLO terms are included in the analysis, while the leading order LECs are stable.

From Figure 2 we can explicitly observe the convergence behavior of the chiral expansion.

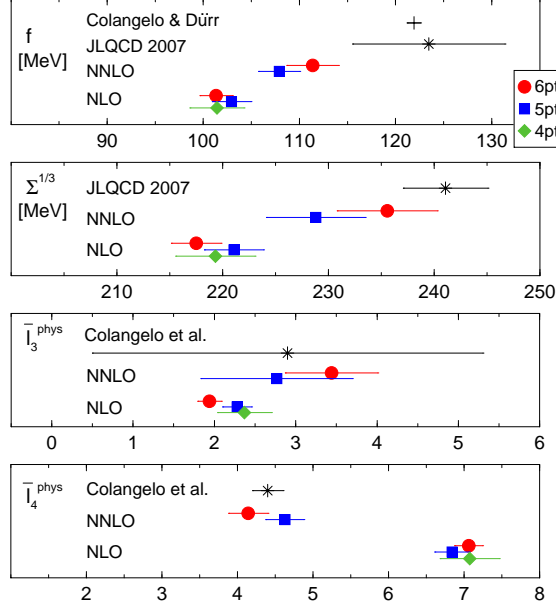


FIG. 3: Comparison of the ChPT parameters obtained from the NLO fit and NNLO fit. Red circles, blue squares and green diamonds are corresponding to the results of the fit using the lightest 4, 5 and all 6 data points. Star symbols represent reference points.

For instance, at the kaon mass region $m_\pi \sim 500$ MeV, the NLO term contributes at a -10% ($+28\%$) level to m_π^2/m_q (f_π), and the correction at NNLO is about $+3\%$ ($+18\%$). At least, the expansion is converging (NNLO is smaller than NLO) for both of these quantities, but quantitatively the convergence behavior depends significantly on the quantity of interest. For f_π the NNLO contribution is already substantial at the kaon mass region.

From the ξ -fit, we extract the LECs of ChPT, *i.e.* the decay constant in the chiral limit f , chiral condensate $\Sigma = Bf^2/2$, and the NLO LECs $\bar{l}_3^{\text{phys}} = -c_3/2B + \ln(4\pi f/m_{\pi^+})^2$ and $\bar{l}_4^{\text{phys}} = c_4/2f + \ln(4\pi f/m_{\pi^+})^2$. For each quantity, a comparison of the results between the NLO and the NNLO fits is shown in Figure 3. In each panel, the results with 5 and 6 lightest data points are plotted for the NNLO fit. The simultaneous fits give χ^2/dof in a reasonable range (below 1.91). For the NLO fits, we plot results obtained with 4, 5 and 6 points to show the stability of the fit. The χ^2/dof is less than 2.24 except for f_π with 4 points, for which it is 3.11. The results for these physical quantities are consistent within either the NLO or the NNLO fit. On the other hand, as seen for \bar{l}_4^{phys} most prominently, there is a significant disagreement between NLO and NNLO. This is due to the large NNLO coefficients as already discussed.

We quote our final results from the NNLO fit with all data points: $f = 111.4(2.7)(^{+0.0}_{-3.5})(^{+6.0}_{-0.0})$ MeV, $\Sigma^{\overline{\text{MS}}}(2 \text{ GeV}) = [235.6(4.9)(^{+0.0}_{-6.7})(^{+12.7}_{-0.0}) \text{ MeV}]^3$, $\bar{l}_3^{\text{phys}} = 3.44(57)(^{+0}_{-68})(^{+32}_{-0})$, and $\bar{l}_4^{\text{phys}} = 4.14(26)(^{+49}_{-0})(^{+32}_{-0})$. From the value at the neutral pion mass $m_{\pi^0} = 135.0$ MeV, we obtain the average up and down quark mass m_{ud} and the pion decay constant as $m_{ud}^{\overline{\text{MS}}}(2 \text{ GeV}) = 4.44(15)(^{+9}_{-0})(^{+0}_{-23})$ MeV and $f_\pi = 119.3(2.4)(^{+0.0}_{-2.8})(^{+6.4}_{-0.0})$ MeV. In these results, the first error is statistical, where the error of the renormalization constant is included in quadrature for $\Sigma^{1/3}$ and m_{ud} , and the second one is systematic due to the chiral fit, which is estimated by the difference from the fit with the lightest 5 data points. For quantities carrying mass dimensions, the third error is from the ambiguity in the determination of r_0 . We estimate these errors from the difference of the results with our input $r_0 = 0.49$ fm and that with 0.465 fm [13]. The third errors for \bar{l}_3^{phys} and \bar{l}_4^{phys} reflect an ambiguity of choosing the renormalization scale of ChPT ($4\pi f$ or $4\pi f_\pi$). There are other possible sources of systematic errors due to the discretization effect, remaining finite volume effect, and the effect of missing strange quark in the sea.

In each panel of Figure 3, we also plot reference points (a plus and stars) for comparison. Overall, with the NNLO fits, we find good agreement with those reference values. For f , our result is significantly lower than the two-loop result in two-flavor ChPT [14], $f = 121.9 \pm 0.7$ MeV, but taking account of the scale uncertainty, which is not shown in the plot, the agreement is more reasonable. For f and $\Sigma^{\overline{\text{MS}}}(2 \text{ GeV})$, we also plot the lattice results from our independent simulation in the ϵ -regime [15]. We observe a good agreement with the NNLO fits. Comparison of the LECs \bar{l}_3^{phys} and \bar{l}_4^{phys} with the phenomenological values [2] also favor the NNLO fits, especially for \bar{l}_4^{phys} .

With the presently available computational power, the chiral extrapolation is still necessary in the lattice QCD calculations. The consistency test of the lattice data with ChPT as described in this paper is crucial for reliable chiral extrapolation of any physical quantities to be calculated on the lattice. With a two-flavor simulation preserving exact chiral symmetry, we demonstrate that the lattice data are well described with the use of the resummed expansion parameter $\xi = m_\pi^2/(4\pi f_\pi)^2$. Extension of the analysis to the case of partially quenched QCD [16] and to other physical quantities, such as the pion form factor [17] is on-going. Also, simulations with exact chiral symmetry including dynamical strange quark are underway [18].

Acknowledgments

Numerical simulations are performed on Hitachi SR11000 and IBM System Blue Gene Solution at High Energy Accelerator Research Organization (KEK) under a support of its Large Scale Simulation Program (Nos. 07-16). HF was supported by Nishina Foundation. This work is supported in part by the Grant-in-Aid of the Ministry of Education (Nos. 17740171, 18034011, 18340075, 18740167, 18840045, 19540286, 19740121, 19740160, 20025010, 20039005, 20340047, 20740156) and the National Science Council of Taiwan (Nos. NSC96-2112-M-002-020-MY3, NSC96-2112-M-001-017-MY3).

-
- [1] J. Gasser and H. Leutwyler, *Ann. Phys.* **158**, 142 (1984).
 - [2] G. Colangelo, J. Gasser, and H. Leutwyler, *Nucl. Phys.* **B603**, 125 (2001), hep-ph/0103088.
 - [3] H. Neuberger, *Phys. Lett.* **B417**, 141 (1998), hep-lat/9707022.
 - [4] H. Neuberger, *Phys. Lett.* **B427**, 353 (1998), hep-lat/9801031.
 - [5] J. Bijnens, G. Colangelo, and P. Talavera, *JHEP* **05**, 014 (1998), hep-ph/9805389.
 - [6] J. Noaki et al. (JLQCD), *PoS LAT2007*, 126 (2007), arXiv:0710.0929 [hep-lat].
 - [7] S. Aoki et al. (JLQCD) (2008), 0803.3197.
 - [8] G. Colangelo, S. Durr, and C. Haefeli, *Nucl. Phys.* **B721**, 136 (2005), hep-lat/0503014.
 - [9] H. Fukaya et al. (JLQCD), *Phys. Rev.* **D74**, 094505 (2006), hep-lat/0607020.
 - [10] R. Brower, S. Chandrasekharan, J. W. Negele, and U. J. Wiese, *Phys. Lett.* **B560**, 64 (2003), hep-lat/0302005.
 - [11] S. Aoki, H. Fukaya, S. Hashimoto, and T. Onogi, *Phys. Rev.* **D76**, 054508 (2007), arXiv:0707.0396 [hep-lat].
 - [12] S. Aoki et al. (JLQCD and TWQCD) (2007), arXiv:0710.1130 [hep-lat].
 - [13] C. Aubin et al. (MILC), *Phys. Rev.* **D70**, 114501 (2004), hep-lat/0407028.
 - [14] G. Colangelo and S. Dür, *Eur. Phys. J.* **C33**, 543 (2004), hep-lat/0311023.
 - [15] H. Fukaya et al. (JLQCD) (2007), arXiv:0711.4965 [hep-lat].
 - [16] S. Aoki et al. (JLQCD), in preparation.
 - [17] T. Kaneko et al. (JLQCD), *PoS LAT2007*, 148 (2007), arXiv:0710.2390 [hep-lat].
 - [18] S. Hashimoto et al. (JLQCD), *PoS LAT2007*, 101 (2007), arXiv:0710.2730 [hep-lat].